Supporting Information

Embedding of FeOOH Nanorods in the Fabrication of Thin Film Nanocomposite (TFN) Membrane for Enhanced Desalination

Pengfei Li[a b], Liming Wang[a], Mingzheng Bao[a],Yu Yong[a], Jilong Han[a]*, and Q. Jason Niu[b c]*

[a] *College of Chemical and Pharmaceutical, Hebei University of Science & Technology, Shijiazhuang 050018, PR China.*

[b.] *State Key Laboratory of Heavy Oil Processing, College of Chemical Engineering, China University of Petroleum (East China), Qingdao, 266580, P. R. China.*

[c.] *Institute for Advanced Study, Shenzhen University, Shenzhen 518060, PR China*

*Corresponding authors

E-mail: hanjilong@hebust.edu.cn (Jilong Han).

E-mail: qjasonniu@szu.edu.cn (Q. Jason Niu).

S1. Materials

Trimesoyl chloride (TMC, >98.0%), anhydrous ferric chloride ($FeCl_3$) and 1,3-phenylenediamine (MPD, >98.0%) were supplied by TCI Chemicals. Hydrochloric acid (HCl, 36.0%), bovine serum albumin (BSA, >98%), sodium chloride (NaCl, 99.5%) were provided by Sinopharm Chemical Reagent Co., Ltd. The polysulfone membrane was commercial products.

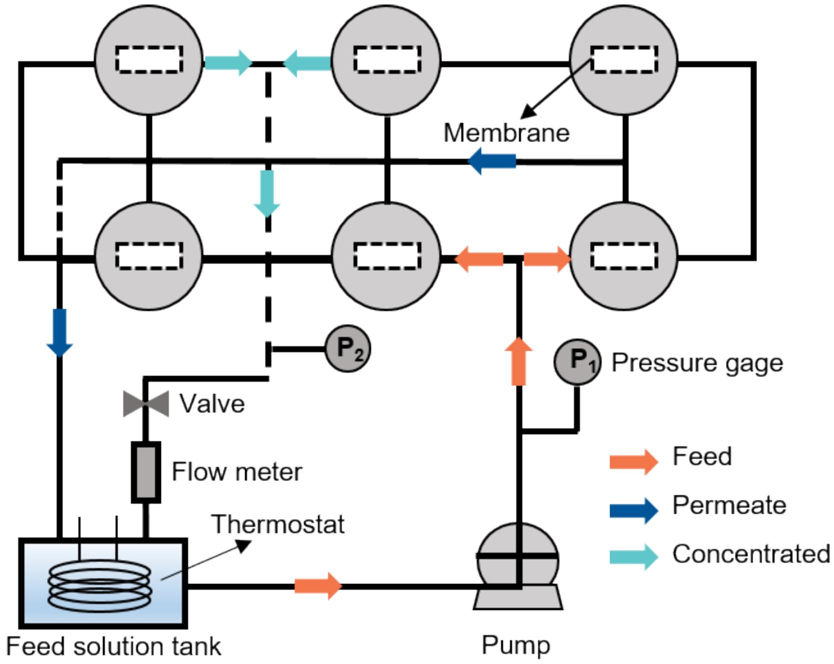

Figure S1. Schematic diagram of cross-flow system test equipment.

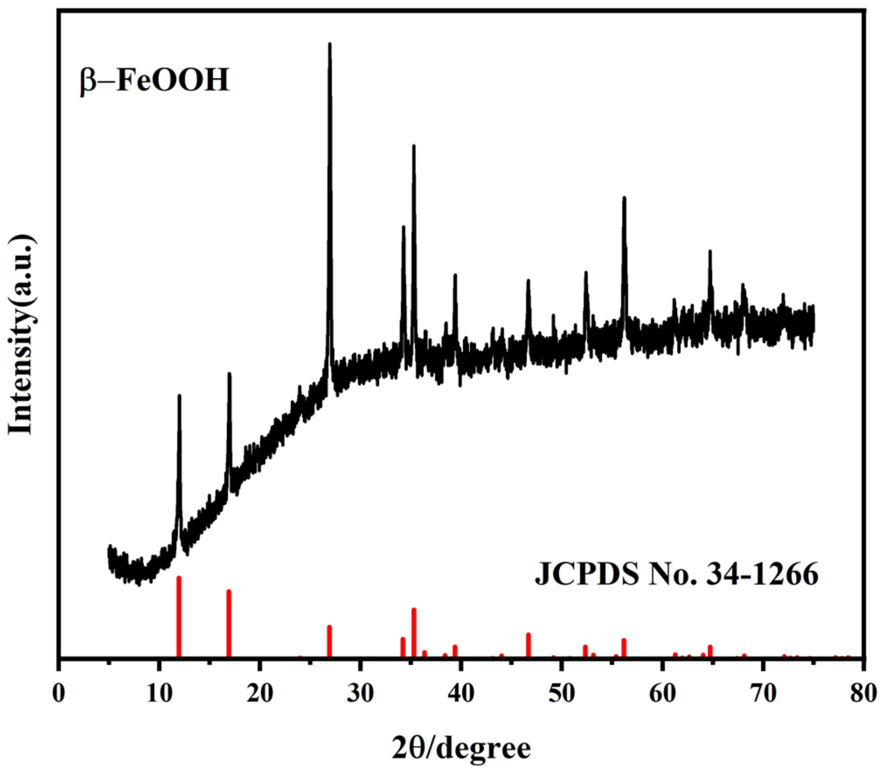

Figure S2. XRD spectra of FeOOH nanorods. The diffraction peaks observed at 12°, 26.9°, 34.1°, 35.3°, 39.4°, 46.6°, and 56.2° correspond to the (110), (310), (400), (211), (301), (411), and (521) crystal planes of β-FeOOH.

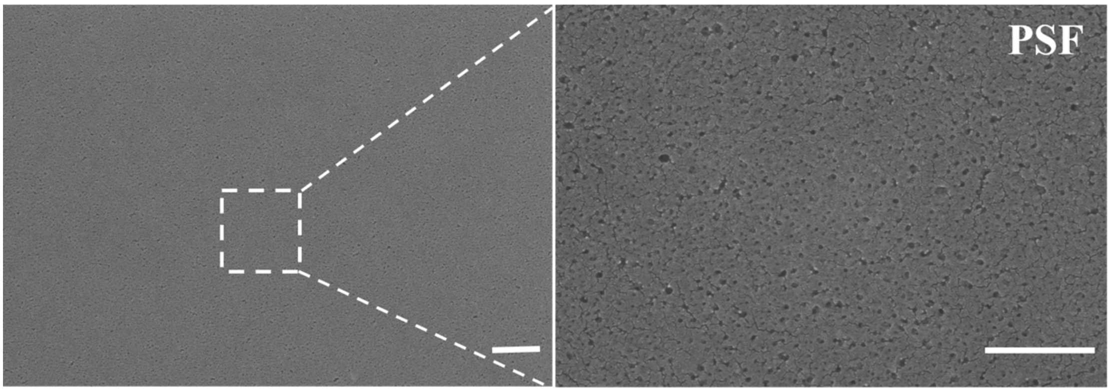

Figure S3. The SEM image of the PSF substrate

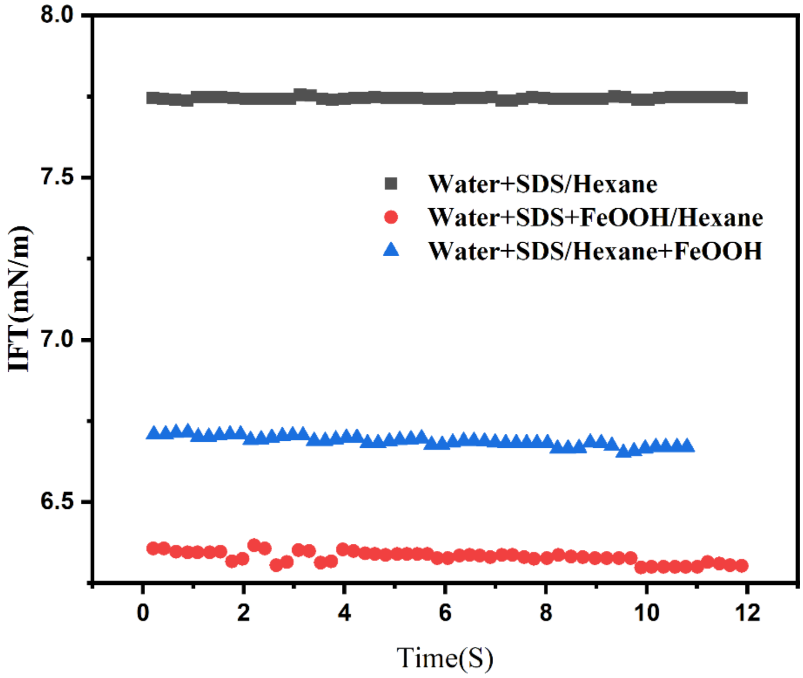

Figure S4. The interfacial tension of three oil-water interface systems.

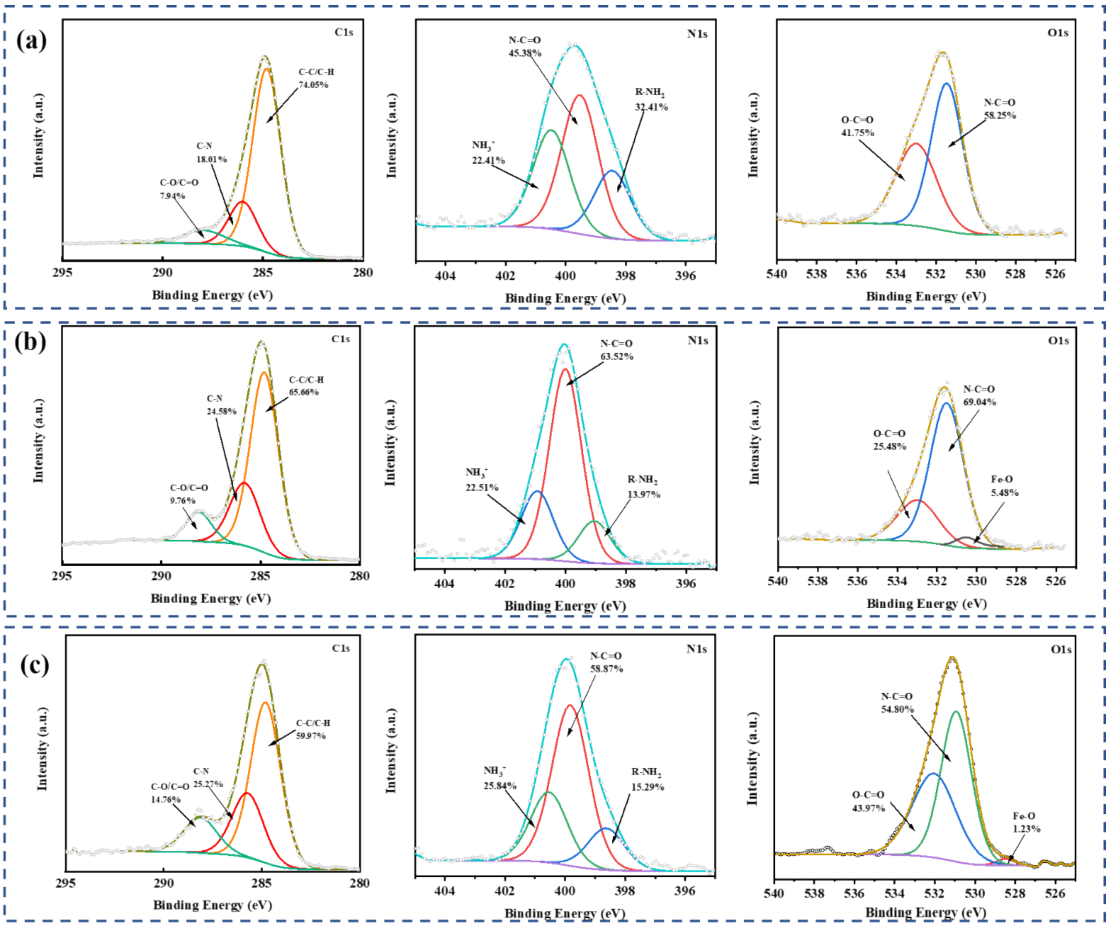

Figure S5 The C1s, N1s and O1s peak of (a) TFC, (b) TFN-O, and (c) TFN-A membranes determined by XPS.

It is well known that the loading of inorganic nanoporous materials has a crucial impact on the performance of nanocomposite membranes. In this study, the effect of different FeOOH nanorod loadings in the aqueous and organic phases on the separation performance was investigated. As shown in Figure S6, FeOOH nanorods at various concentrations were uniformly dispersed in the MPD aqueous solution using ultrasonic dispersion. With increasing FeOOH nanorod content, the permeance of the TFN-A membranes increased. When the FeOOH concentration was increased from 0 wt% to 0.015 wt%, the NaCl rejection remained largely unchanged. However, at concentrations exceeding 0.015 wt%, a decline in rejection was observed, with TFN-A membranes containing 0.02 wt% FeOOH nanorods exhibiting a NaCl rejection of 96%. This reduction in rejection is likely due to the aggregation of FeOOH nanorods at higher concentrations, which disrupts the formation of a dense polyamide selective layer during interfacial polymerization. This trade-off between increased flux and decreased rejection has been similarly reported in other studies. Based on these results, the optimal FeOOH nanorod loading in the aqueous phase was determined to be 0.015 wt%.

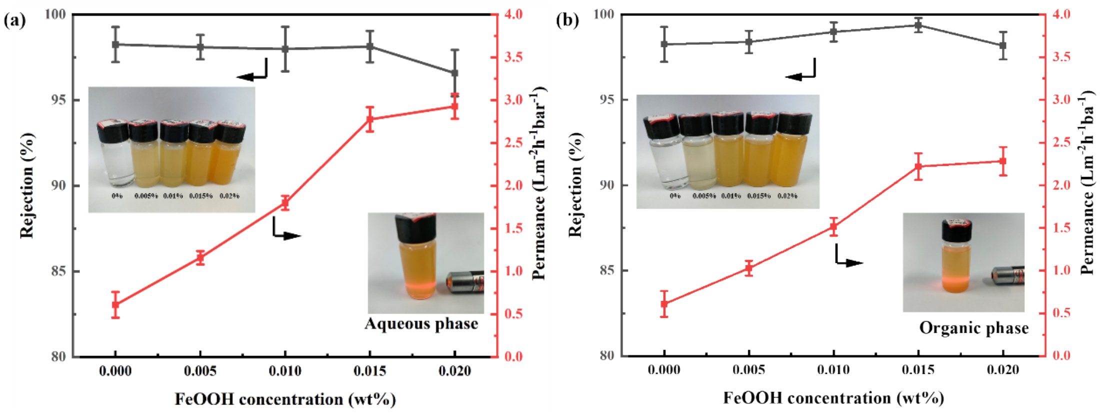

Figure S6 Effect of different concentrations of FeOOH in aqueous phase (a) and organic phase (b) on desalination performance of TFN membranes

FeOOH nanorods at various concentrations were also uniformly dispersed in the TMC organic phase via ultrasonic treatment. The influence of different FeOOH nanorod concentrations in the organic phase on desalination performance is illustrated in Figure 3b. As shown, the permeance of the TFN-O membranes increased gradually with increasing FeOOH content. However, when the FeOOH concentration reached 0.02 wt%, further increases in flux became negligible. In contrast to the TFN-A membranes where FeOOH nanorods were incorporated into the aqueous phase, the NaCl rejection of the TFN-O membranes slightly improved as the FeOOH concentration in the organic phase increased to 0.015 wt%. At a FeOOH concentration of 0.02 wt%, a slight decrease in salt rejection was observed, though the NaCl rejection remained above 98%. To enable a systematic comparison between the two types of TFN membranes, those prepared with the FeOOH loading of 0.015 wt% in the organic phase were selected for further experimental studies.

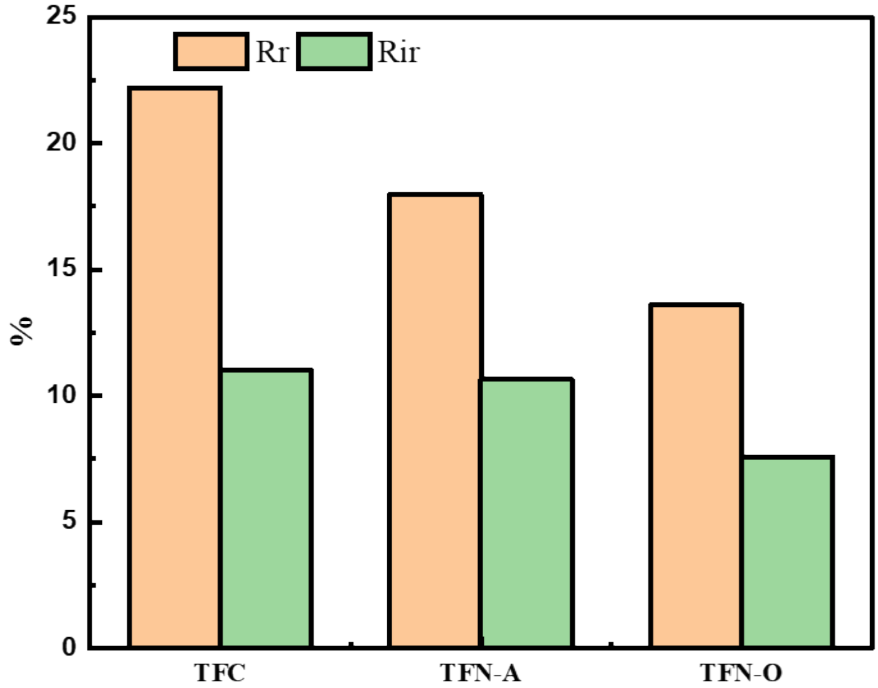

Figure S7 Reversible and irreversible fouling ratios of different reverse osmosis membranes.

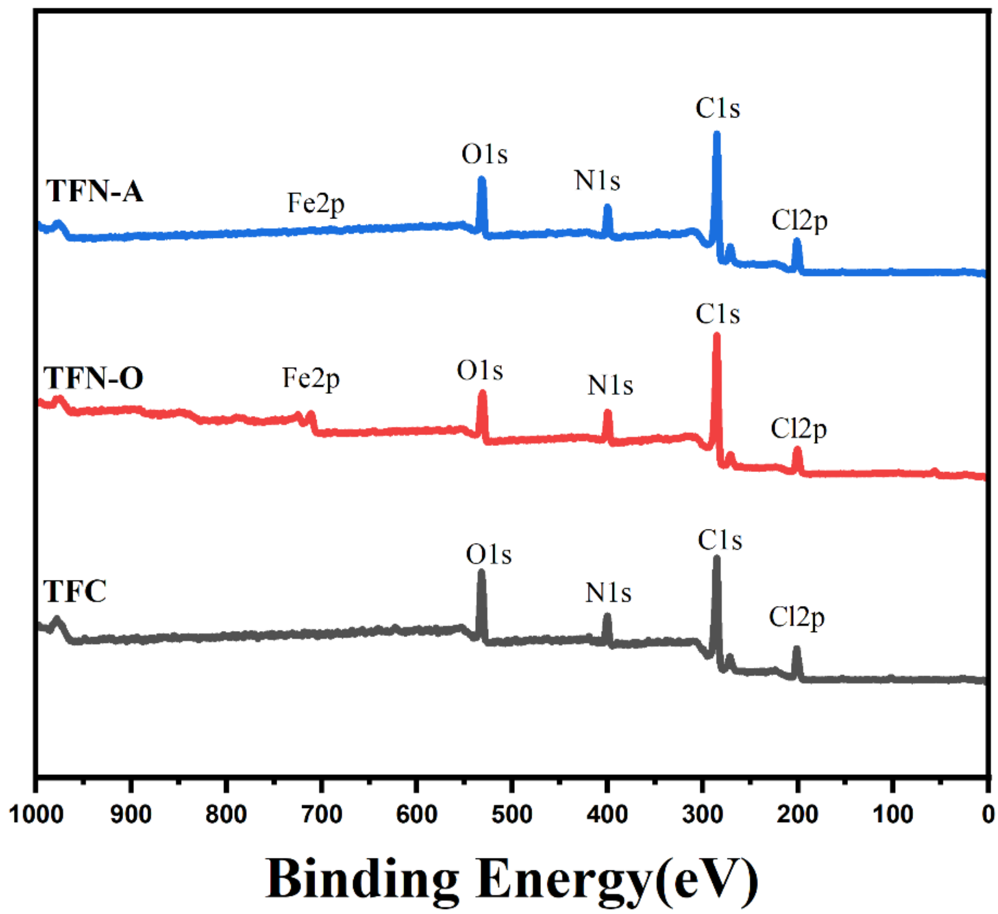

Figure S8 XPS spectra of the TFC, TFN-A, and TFN-O membranes after the chlorination test.

Table S1 Elemental compositions and the O/N ratio of the TFC, TFN-A and TFN-O membranes after the chlorination test

Membrane	C (%)	O (%)	N (%)	Fe (%)	Cl (%)	O/N
TFC	66.21	15.81	10.77	0	7.22	1.46
TFN-A	68.74	12.48	11.19	0.6	6.98	1.12
TFN-O	68.03	12.08	11.74	2.63	5.52	1.03

Table S2 Comparison of permeance and rejection of the state-of-the-art TFN membranes.

Nanomaterials	NaCl/ppm & pressure/bar[1]	A/O	Water permeance LMH bar^{-1}	Permeability ($Lm^{-2}h^{-1}bar^{-1}$ $m\times10^{-5}$)	A/B	[a] Water permeance increase rate/%	*R*%	[b] *R*% increase rate/%
[c] FeOOH	2000/15.5	A	2.78	10.44	3.80	355.74 ± 6.67	98.13 ±1.02	-0.12
[c] FeOOH	2000/15.5	O	2.22	7.27	11.61	263.93 ± 2.56	99.38 ±0.42	1.13
TFC	2000/15.5	-	0.61	1.13	4.06	-	98.25 ±0.92	-
pU-66[1]	2000/15.5	O	4.30	10.32	4.7	72	98.5	1
ZIF-L[2]	2000/15.5	i	5.3	0.61	1.61	53.6	96.3	-1.95
$TpPa_2CN$[3]	1000/6	A	1.9	2.47	8.16	139.5	97.68	1.4
ZIF-8[4]	2000/15.5	i	3.64	4.37	5.10	267.7	98.6	-0.1
ZIF-8[5]	2000/15.5	A	4.0	10.0	8.98	43.1	99.2	0.3
ZIF-8[6]	2000/15.5	O	3.4	3.4	4.75	161.7	98.5	0.4
TiO_2[7]	2000/7.6	A	3.4	1.19	30.6	49.3	99.45	2.1
SiO_2[8]	11000/44	A	1.1	1.10	0.25	55.6	90	-1.1
SiO_2[9]	2000/20.7	O	2.3	11.5	2.05	64.6	97.5	-1.0
SiO_2[10]	2000/16	O	3.3	9.9	1.67	178.6	96	0.0
SiO_2[11]	2000/5	i	9.7	1.94	8.33	102.1	96.5	-1.5
CNTs-M/MO[12]	2000/10	i	1.2	4.08	1.22	114.8	91	1.2
CNTs[13]	2000/15.5	A	3.0	6.0	0.83	34.8	92	1.1
MWCNTs[14]	2000/16	A	1.8	2.7	0.62	88.2	90	-6.3
CNTa/GO[14]	2000/15.5	A	2.9	5.8	2.19	19.3	96.8	-0.4
GO[14]	2000/15.5	A	2.5	2.2	7.17	5.8	97	-0.5
GO[15]	2000/15.5	A	1.1	5.0	2.34	81.5	99	-0.1
GO[16]	1000/15	coat	2.7	2.73	1.34	-11.1	95	-1.6
GOQD[17]	2000/16	A	2.3	4.6	5.75	52.5	98.8	0.3
N-GOQD[18]	2000 /15	A	1.8	4.5	0.88	150.0	92.1	-1.1
$g-C_3N_4$[19]	2000/15.5	A	3.0	9.0	24.06	22.4	99.7	1.7
HNTs[20]	2000/15	O	2.4	4.8	1.63	90.5	95.6	-1.6
NH_2-TNTs[21]	2000/15	O	3.9	7.8	0.10	92.1	58	2.6
NaX-Zeolite[22]	2000/12	O	1.2	1.92	1.84	79.0	95	-2.1
NaA-Zeolite[23]	2000/12	A	2.2	3.3	0.62	71.1	86.5	-5.4

Ag[24]	2000/20.68	coat	3.4	6.8	0.77	39.8	93.6	-2.4
ZnO[25]	1753/15.5	O	2.1	6.3	1.74	22.6	96	-2.0
MoS_2[26]	2000 /15.5	O	6.2	11.1	4.75	20.2	98.5	0.5
CNCs[27]	3000/20	O	3.2	8.64	2.55	110.0	97.8	0.7
UiO-66[28]	2000/15.5	O	3.7	8.62	11.07	50.4	99.35	0.3
Ti_3C_2Tx–TA[29]	2000/20	A	2.4	8.81	1.30	41.2	96.0	-2.5
Ti_3C_2Tx[30]	2000/16	A	2.53	9.48	4.59	41.2	98.5	0.25
CNF[31]	2000/15	A	2.98	8.94	1.9	49.7	96.2	-2.05
CeO_2[32]	2000/16	A	2.75	7.15	3.42	50.27	98	-0.7
Al_2O_3[33]	2000/10	O	6.75	16.2	5.9	138	98	-0.25
[d] LG Nano H_2O[5]	2000/15.5	O	3.0	9.0	28.89	391.80	99.75	0.015
[e] Dow-SW30HR[5]	2000/15.5		1.1	1.10	11.99	83.02	99.4	0.012
[e] BW30[5]	2000/15.5		2.1	2.10	5.10	244.26	98.6	0.0035
[e] Sepro-RO4[5]	2000/15.5		1.0	1.00	5.96	63.93	98.8	0.0055

[a] Water permeance increase rate (%) = (*P*w(TFN)-*P*w(TFC))/*P*w(TFC) x 100%.

[b] NaCl rejection increase rate (%) = *R*(TFN)-*R*(TFC).

[c] TFC and TFN RO membranes in this work.

[d] The commercial TFN RO membrane.

[e] The commercial TFC RO membranes.

References

[1] Lee, B.K., et al., Enhanced reverse osmosis performance via amphiphilic polyMOF embedded thin-film nanocomposite membranes, Desalination. 598 (2025) 118407 https://doi.org/10.1016/j.desal.2024.118407

[2] Zhao, S., et al., Ultrafast Water Transport of Reverse Osmosis Membrane Based on Quasi-Vertically Oriented, Nano Letters, 24(45) (2024) 14329-14336.https://doi.org/10.1021/acs.nanolett.4c04033

[3] L. Xu, B. Shan, C. Gao, J. Xu, Multifunctional thin-film nanocomposite membranes comprising covalent organic nanosheets with high crystallinity for efficient reverse osmosis desalination, Journal of Membrane Science 593 (2020) 117398. https://doi.org/10.1016/j.memsci.2019.117398

[4] Z. Zhai, N. Zhao, W. Dong, P. Li, H. Sun, Q.J. Niu, In Situ Assembly of a Zeolite Imidazolate Framework Hybrid Thin-Film Nanocomposite Membrane with Enhanced Desalination Performance Induced by Noria–Polyethyleneimine Codeposition, ACS Applied Materials & Interfaces 11(13) (2019) 12871-12879. https://doi.org/10.1021/acsami.9b01237

[5] T.H. Lee, J.Y. Oh, S.P. Hong, J.M. Lee, S.M. Roh, S.H. Kim, H.B. Park, ZIF-8 particle size effects on reverse osmosis performance of polyamide thin-film nanocomposite membranes: Importance of particle deposition, Journal of Membrane Science 570 (2019) 23-33. https://doi.org/10.1016/j.memsci.2018.10.015

[6] J. Duan, Y. Pan, F. Pacheco, E. Litwiller, Z. Lai, I. Pinnau, High-performance polyamide thin-film-nanocomposite reverse osmosis membranes containing hydrophobic zeolitic imidazolate framework-8,

Journal of Membrane Science 476 (2015) 303-310. https://doi.org/10.1016/j.memsci.2014.11.038
[7] M. Safarpour, A. Khataee, V. Vatanpour, Thin film nanocomposite reverse osmosis membrane modified by reduced graphene oxide/TiO_2 with improved desalination performance, Journal of Membrane Science 489 (2015) 43-54. https://doi.org/10.1016/j.memsci.2015.04.010
[8] A. Peyki, A. Rahimpour, M. Jahanshahi, Preparation and characterization of thin film composite reverse osmosis membranes incorporated with hydrophilic SiO_2 nanoparticles, Desalination 368 (2015) 152-158. https://doi.org/10.1016/j.desal.2014.05.025
[9] J. Yin, E.-S. Kim, J. Yang, B. Deng, Fabrication of a novel thin-film nanocomposite (TFN) membrane containing MCM-41 silica nanoparticles (NPs) for water purification, Journal of Membrane Science 423 (2012) 238-246. https://doi.org/10.1016/j.memsci.2012.08.020
[10] M. Bao, G. Zhu, L. Wang, M. Wang, C. Gao, Preparation of monodispersed spherical mesoporous nanosilica–polyamide thin film composite reverse osmosis membranes via interfacial polymerization, Desalination 309 (2013) 261-266. https://doi.org/10.1016/j.desal.2012.10.028
[11] H. Shen, S. Wang, H. Xu, Y. Zhou, C. Gao, Preparation of polyamide thin film nanocomposite membranes containing silica nanoparticles via an in-situ polymerization of $SiCl_4$ in organic solution, Journal of Membrane Science 565 (2018) 145-156. https://doi.org/10.1016/j.memsci.2018.08.016
[12] S. Al Aani, A. Haroutounian, C.J. Wright, N. Hilal, Thin Film Nanocomposite (TFN) membranes modified with polydopamine coated metals/carbon-nanostructures for desalination applications, Desalination 427 (2018) 60-74. https://doi.org/10.1016/j.desal.2017.10.011
[13] H.J. Kim, K. Choi, Y. Baek, D.-G. Kim, J. Shim, J. Yoon, J.-C. Lee, High-performance reverse osmosis CNT/polyamide nanocomposite membrane by controlled interfacial interactions, ACS Applied Materials &Interfaces 6(4) (2014) 2819-2829. https://doi.org/10.1021/am405398f
[14] H.J. Kim, M.-Y. Lim, K.H. Jung, D.-G. Kim, J.-C. Lee, High-performance reverse osmosis nanocomposite membranes containing the mixture of carbon nanotubes and graphene oxides, Journal of Materials Chemistry A 3(13) (2015) 6798-6809. https://doi.org/10.1039/C4TA06080F
[15] H.-R. Chae, J. Lee, C.-H. Lee, I.-C. Kim, P.-K. Park, Graphene oxide-embedded thin-film composite reverse osmosis membrane with high flux, anti-biofouling, and chlorine resistance, Journal of Membrane Science 483 (2015) 128-135. https://doi.org/10.1016/j.memsci.2015.02.045
[16] F. Shao, L. Dong, H. Dong, Q. Zhang, M. Zhao, L. Yu, B. Pang, Y. Chen, Graphene oxide modified polyamide reverse osmosis membranes with enhanced chlorine resistance, Journal of Membrane Science 525 (2017) 9-17. https://doi.org/10.1016/j.memsci.2016.12.001
[17] X. Song, Q. Zhou, T. Zhang, H. Xu, Z. Wang, Pressure-assisted preparation of graphene oxide quantum dot-incorporated reverse osmosis membranes: antifouling and chlorine resistance potentials, Journal of Materials Chemistry A 4(43) (2016) 16896-16905. https://doi.org/10.1039/C6TA06636D
[18] M. Fathizadeh, H.N. Tien, K. Khivantsev, Z. Song, F. Zhou, M. Yu, Polyamide/nitrogen-doped graphene oxide quantum dots (N-GOQD) thin film nanocomposite reverse osmosis membranes for high flux desalination, Desalination 451 (2019) 125-132. https://doi.org/10.1016/j.desal.2017.07.014
[19] S.S. Shahabi, N. Azizi, V. Vatanpour, Synthesis and characterization of novel g-C_3N_4 modified thin film nanocomposite reverse osmosis membranes to enhance desalination performance and fouling resistance, Separation and Purification Technology 215 (2019) 430-440.

https://doi.org/10.1016/j.seppur.2019.01.031
[20] M. Ghanbari, D. Emadzadeh, W. Lau, T. Matsuura, A. Ismail, Synthesis and characterization of novel thin film nanocomposite reverse osmosis membranes with improved organic fouling properties for water desalination, Rsc Advances 5(27) (2015) 21268-21276. https://doi.org/10.1039/C4RA16177G
[21] D. Emadzadeh, W. Lau, M. Rahbari-Sisakht, A. Daneshfar, M. Ghanbari, A. Mayahi, T. Matsuura, A. Ismail, A novel thin film nanocomposite reverse osmosis membrane with superior anti-organic fouling affinity for water desalination, Desalination 368 (2015) 106-1. https://doi.org/10.1016/j.desal.2014.11.019
[22] M. Fathizadeh, A. Aroujalian, A. Raisi, Effect of added NaX nano-zeolite into polyamide as a top thin layer of membrane on water flux and salt rejection in a reverse osmosis process, Journal of Membrane Science 375(1-2) (2011) 88-95. https://doi.org/10.1016/j.memsci.2011.03.017
[23] H. Huang, X. Qu, H. Dong, L. Zhang, H. Chen, Role of NaA zeolites in the interfacial polymerization process towards a polyamide nanocomposite reverse osmosis membrane, Rsc Advances 3(22) (2013) 8203-8207. https://doi.org/10.1039/C3RA40960K
[24] J. Yin, Y. Yang, Z. Hu, B. Deng, Attachment of silver nanoparticles (AgNPs) onto thin-film composite (TFC) membranes through covalent bonding to reduce membrane biofouling, Journal of Membrane Science 441 (2013) 73-82. https://doi.org/10.1016/j.memsci.2013.03.060
[25] A. Al-Hobaib, J. El Ghoul, I. Ghiloufi, L. El Mir, Synthesis and characterization of polyamide thin-film nanocomposite membrane reached by aluminum doped ZnO nanoparticles, Materials Science in Semiconductor Processing 42 (2016) 111-114. https://doi.org/10.1016/j.mssp.2015.07.058
[26] Y. Li, S. Yang, K. Zhang, B. Van der Bruggen, Thin film nanocomposite reverse osmosis membrane modified by two dimensional laminar MoS_2 with improved desalination performance and fouling-resistant characteristics, Desalination 454 (2019) 48-58. https://doi.org/10.1016/j.desal.2018.12.016
[27] F. Asempour, D. Emadzadeh, T. Matsuura, B. Kruczek, Synthesis and characterization of novel Cellulose Nanocrystals-based Thin Film Nanocomposite membranes for reverse osmosis applications, Desalination 439 (2018) 179-187. https://doi.org/10.1016/j.desal.2018.04.009
[28] L. Liu, X. Xie, S. Qi, R. Li, X. Zhang, X. Song, C. Gao, Thin film nanocomposite reverse osmosis membrane incorporated with UiO-66 nanoparticles for enhanced boron removal, Journal of Membrane Science 580 (2019) 101-109. https://doi.org/10.1016/j.memsci.2019.02.072
[29] K. Zarshenas, H. Dou, S. Habibpour, A. Yu, Z. Chen, Thin Film Polyamide Nanocomposite Membrane Decorated by Polyphenol-Assisted Ti_3C_2T x MXene Nanosheets for Reverse Osmosis, ACS Applied Materials & Interfaces 14(1) (2021) 1838-1849. https://doi.org/10.1021/acsami.1c16229
[30] X. Wang, Q. Li, J. Zhang, H. Huang, S. Wu, Y. Yang, Novel thin-film reverse osmosis membrane with MXene Ti_3C_2Tx embedded in polyamide to enhance the water flux, anti-fouling and chlorine resistance for water desalination, Journal of Membrane Science 603 (2020) 118036. https://doi.org/10.1016/j.memsci.2020.118036
[31] S. Liu, Z.-X. Low, H.M. Hegab, Z. Xie, R. Ou, G. Yang, G.P. Simon, X. Zhang, L. Zhang, H. Wang, Enhancement of desalination performance of thin-film nanocomposite membrane by cellulose nanofibers, Journal of Membrane Science 592 (2019) 117363. https://doi.org/10.1016/j.memsci.2019.117363

[32] Y. Wang, B. Gao, S. Li, B. Jin, Q. Yue, Z. Wang, Cerium oxide doped nanocomposite membranes for reverse osmosis desalination, Chemosphere, 218 (2019) 974-983. https://doi.org/10.1016/j.chemosphere.2018.11.207

[33] Kotp, Y.H., High-flux TFN nanofiltration membranes incorporated with Camphor-Al_2O_3 nanoparticles for brackish water desalination. Chemosphere, 265 (2021) 128999. https://doi.org/10.1016/j.chemosphere.2020.128999

[34] Lee T. H., Oh J. Y., Hong S. P., et al. ZIF-8 particle size effects on reverse osmosis performance of polyamide thin-film nanocomposite membranes: Importance of particle deposition[J]. Journal of Membrane Science, 570 (2019) 23-33. https://doi.org/10.1016/j.memsci.2018.10.015

[35] Jiang, C., et al., Ultrathin Film Composite Membranes Fabricated by Novel In Situ Free Interfacial Polymerization for Desalination. ACS Applied Materials & Interfaces, 12(22) (2020) 25304-25315.https://doi.org/10.1021/acsami.0c05166

[36] Zhao, S., et al., Ultrafast Water Transport of Reverse Osmosis Membrane Based on Quasi-Vertically Oriented.NanoLetters, 24(45) (2024) 14329-14336.https://doi.org/10.1021/acs.nanolett.4c04033

[37] Yuan, B., et al., ZIF-8 ligand exchange-driven fabrication of high-permeability reverse osmosis membranes for desalination and small molecule pollutant removal. Separation and Purification Technology, 377(3) (2025) 134457.https://doi.org/10.1016/j.seppur.2025.134457